



Published in final edited form as:

Lab Invest. 2015 May ; 95(5): 515–524. doi:10.1038/labinvest.2015.29.

Involvement of hepatic stellate cell cytoglobin in acute hepatocyte damage through the regulation of CYP2E1-mediated xenobiotic metabolism

Yuga Teranishi^{1,5}, Tsutomu Matsubara^{2,5}, Kristopher W Krausz³, Thi TT Le¹, Frank J Gonzalez³, Katsutoshi Yoshizato^{1,4}, Kazuo Ikeda², and Norifumi Kawada¹

¹Department of Hepatology, Graduate School of Medicine, Osaka City University, Osaka, Japan

²Department of Anatomy and Regenerative Biology, Graduate School of, Medicine, Osaka City University, Osaka, Japan

³Laboratory of Metabolism, Center for Cancer Research, National Cancer Institute, National Institutes of Health, Bethesda, MD, USA

⁴Phoenixbio Co., Ltd, Hiroshima, Japan

Abstract

Oxygen (O₂) is required for cytochrome P450 (CYP)-dependent drug metabolism. Cytoglobin (*CYGB*) is a unique globin expressed exclusively in hepatic stellate cells (HSCs). However, its role in O₂-dependent metabolism in neighboring hepatocytes remains unknown. This study provides evidence that *CYGB* in HSCs is involved in acetaminophen (*N*-acetyl-*p*-aminophenol; APAP)-induced hepatotoxicity. Serum alanine aminotransferase levels were higher in wild-type mice than in *CYGB*-null mice. Wild-type mice exhibited more severe hepatocyte necrosis around the central vein area compared with *CYGB*-null mice, thus indicating that *CYGB* deficiency protects against APAP-induced liver damage. Although no difference in the hepatic expression of CYP2E1, a key enzyme involved in APAP toxicity, was observed between wild-type and *CYGB*-null mice, the serum levels of the APAP metabolites cysteinyl-APAP and *N*-acetyl-cysteinyl-APAP were decreased in *CYGB*-null mice, suggesting reduced APAP metabolism in the livers of *CYGB*-null mice. In primary cultures, APAP-induced hepatocyte damage was increased by co-culturing with wild-type HSCs but not with *CYGB*-null HSCs. In addition, cell damage was markedly alleviated under low O₂ condition (5% O₂), suggesting the requirement of O₂ for APAP toxicity. Carbon tetrachloride-induced liver injury (CYP2E1-dependent), but not lipopolysaccharide/ D-galactosamine-induced injury (CYP2E1-independent), was similarly alleviated in *CYGB*-null mice. Considering the function of *CYGB* as O₂ carrier, these results

Correspondence: Professor N Kawada, MD, PhD, Department of Hepatology, Graduate School of Medicine, Osaka City University, 1-4-3, Asahimachi, Abeno, Osaka 545-8585, Japan, kawadanori@med.osaka-cu.ac.jp.

⁵These authors contributed equally to this work.

AUTHOR CONTRIBUTIONS

YT, TM, and NK conceived and designed the experiments. KWK and FJG quantified the APAP metabolites. LT provided technical assistance in the isolation of hepatocytes and HSCs. KI and KY contributed critically to the design of the manuscript in terms of important intellectual content. YT, TM, and NK wrote the manuscript, with suggestions from all authors.

DISCLOSURE/CONFLICT OF INTEREST

The authors declare no conflict of interest.

Supplementary Information accompanies the paper on the Laboratory Investigation website (<http://www.laboratoryinvestigation.org>)

strongly support the hypothesis that HSCs are involved in the CYP2E1-mediated xenobiotic activation by augmenting O₂ supply to hepatocytes. In conclusion, *CYGB* in HSCs contributes to the CYP-mediated metabolism of xenobiotics in hepatocytes by supplying O₂ for enzymatic oxidation.

The metabolism of xenobiotics, including clinical drugs, occurs primarily in the liver. Most xenobiotic detoxification metabolism involves cytochrome P450 (CYP) enzymes, which are predominantly expressed in the liver,¹ and these processes occasionally result in acute hepatocyte damage. For instance, acetaminophen (*N*-acetyl-*p*-aminophenol; APAP) and carbon tetrachloride (CCl₄) are metabolized by CYP to generate toxic intermediates.

APAP is commonly used as an antipyretic and analgesic drug. CYP-mediated APAP metabolism is known to generate *N*-acetyl-*p*-benzoquinone imine (NAPQI), which binds to cellular macromolecules and initiates hepatocyte damage if present at high concentrations under glutathione (GSH) depletion.² CYP1A2, CYP2A6, CYP2E1, and CYP3A have been identified as enzymes that generate NAPQI from APAP.³ Among these CYPs, CYP2E1 has the lowest *K_m* for APAP, and the CYP2E1-dependent metabolism of APAP can result in hepatotoxicity.⁴ CYP2E1 is a monooxygenase that requires molecular oxygen (O₂) for its enzymatic activity. A recent study reported that the APAP-induced damage to primary mouse hepatocytes was reduced under a low O₂ concentration (5% O₂) compared with normoxic conditions (20% O₂).⁵ Thus, APAP-induced acute liver injury may be dependent on hepatic O₂ levels.

The aerobic metabolism of mammals relies on respiratory proteins that function in the transport and storage of O₂. Four globin proteins are known to contribute to O₂ homeostasis in mammals.^{6,7} Hemoglobin in erythrocytes has an important role in the transport of O₂ from the bloodstream to the viscera. In the viscera, myoglobin, neuroglobin, and cytoglobin (CYGB) act as local O₂-binding molecules that facilitate the intracellular diffusion of O₂.⁸ Notably, CYGB in mammals is expressed in various organs, including the liver, heart, brain, and the lung. CYGB is a hexacoordinated heme-containing protein that is able to bind O₂, nitric oxide, and carbon monoxide.^{9,10} CYGB expression increases in response to the duration and severity of hypoxia.¹¹ Thus, CYGB is thought to be an O₂ sensor for the local storage and transport of O₂; however, its contribution to O₂-dependent xenobiotic metabolism remains unclear.

CYGB is a unique globin expressed exclusively in hepatic stellate cells (HSCs), which represent ~5–8% of the cells in the liver.¹² When liver injury occurs, HSCs undergo activation and acquire myofibroblastic characteristics, including increased collagen production. Such characteristic alterations of HSCs are believed to be strongly associated with hepatic fibrosis and the development of liver cirrhosis and cancer. In addition, interactions between hepatocytes and HSCs, as well as the involvement of HSCs in hepatic tissue growth and regeneration have been reported.^{13,14} However, the interplay between HSCs and hepatocytes in drug metabolism remains uncharacterized. Furthermore, the effect of CYGB in HSCs (HSC-CYGB) on APAP-induced acute liver injury has never been investigated.

In this study, the correlation between HSC-CYGB and xenobiotic-mediated hepatocyte injury was investigated *in vivo* and *in vitro* using *Cygb-null* mice. The results implied that a CYGB deficiency in HSCs can regulate hepatic O₂ levels and can alleviate the acute liver injury induced by APAP and CCl₄, by decelerating CYP2E1 metabolism in hepatocytes.

MATERIALS AND METHODS

Materials

All reagents were obtained from Sigma-Aldrich (St Louis, MO, USA) or Wako Pure Chemical (Osaka, Japan), unless otherwise noted.

Mouse Studies

Eight- to 12-week-old male C57BL/6 mice were purchased from Japan SLC (Shizuoka, Japan). *Cygb*-null mice were generated in our laboratory as previously described.¹⁵ *Cygb*-null mice were compared with their wild-type littermates. All mice were cared for according to the guidelines approved by the Institutional Animal Care and Use Committee of Osaka City University, Osaka, Japan. Before APAP treatment, the mice were fasted for 16 h. APAP dissolved in isotonic saline at 65 °C was intraperitoneally (i.p.) injected (300 mg/kg) into mice, which were killed 6 h later. In the study of CCl₄-induced acute liver injury, mice were i.p. injected with CCl₄ (0.5 mg/kg) suspended in corn oil, fasted, and killed 24 h after the injection. Another group of mice were administered D-galactosamine (D-GalN; 700 mg/kg) and lipopolysaccharide (LPS; 5 µg/kg, *Escherichia coli* 0111 :B4) suspended in saline and were killed 6 h later. Blood and liver tissues were collected and stored at — 80 °C for subsequent analysis. For histopathological analysis, small pieces of the liver were fixed in 4% formaldehyde overnight and embedded in paraffin. The liver tissue was sectioned at 5-µm thickness and stained with hematoxylin and eosin. Relative necrotic area (%) was estimated by using Image J software.

Isolation, Fractionation, and Culture of Liver Cells

Hepatocytes and HSCs were isolated from male C57BL/6 mice as previously described.¹⁶ APAP (2.5, 5, 10, 20, or 30 mM) was dissolved in William's Medium E (Gibco, Grand Island, NY) at 65 °C. Hepatocytes were plated in 12- or 24-well plates (1 × 10⁵ cells/ml) (Celltight C-1 Collagen-I, Sumitomo Bakelite, Tokyo, Japan) and were pre-incubated in William's Medium E supplemented with 10% fetal bovine serum (Gibco) and 0.1 µM dexamethasone for 3h before APAP treatment. For co-culture experiments, HSCs (5 × 10⁵ cells/well) were plated in cell culture inserts (Transparent PET membrane, 1.0 µm pore size; Corning, Corning, NY, USA) and incubated overnight in the William's Medium E before co-culture with hepatocytes. The cells were incubated for 16 h with APAP-containing media under a 5% or 20% O₂ atmosphere. Conditioned media derived from the 16-h culture of wild-type or *Cygb*-null HSCs were also used.

Measurement of ALT Activity and APAP Metabolites in Serum

Serum alanine aminotransferase (ALT) activity was determined using a kinetic test (SRL, Tokyo, Japan). The levels of APAP and its metabolites in sera collected 2 h after APAP injection were quantified as previously reported.⁴

Visualization of Hypoxia With Pimonidazole

Mice were injected with APAP (300 mg/kg, i.p.), followed by the administration of pimonidazole hydrochloride (60 mg/kg, i.p.; Hypoxyprobe, Burlington, MA, USA) 1 h before being killed. Small liver pieces were fixed in 4% paraformaldehyde and embedded in paraffin. Paraffin sections (5 μ m) were prepared in the Central Laboratory of the Osaka City University Medical School. Pimonidazole was detected using a Hypoxyprobe-1 Plus Kit, according to the manufacturer's instructions. An anti-fluorescein antibody conjugated to Texas Red (Ab6654; Abcam, Cambridge, UK) was used to visualize the reaction.

GSH Measurements

Liver tissues (100 mg) were homogenized in 1 ml of ice-cold phosphate-buffered saline containing 1 mM EDTA (pH 7.5) and were centrifuged at 10 500 *g* for 15 min at 4 °C. The supernatants were collected and the GSH content in each sample was determined using a GSH quantification kit (Dojindo, Kumamoto, Japan).

Quantitative Real-Time Reverse Transcription-PCR Analyses

Total RNA was isolated using TRIzol reagent (Invitrogen, Carlsbad, CA). cDNA was generated with random hexamer primers (Invitrogen) and the SuperScript RT II enzyme (Invitrogen). Quantitative PCRs were performed using the ABI 5500 Real-Time PCR System (Applied Biosystems, Foster City, CA, USA). The primers used are listed in Supplementary Table 1. Relative expression levels were calculated using the comparative CT method. The expression levels were normalized to that of 18S ribosomal RNA.

Western Blotting

Liver tissues were homogenized with RIPA buffer (50 mM Tris-HCl pH 8.0, 150 mM NaCl, 1% Triton X-100, 1% SDS) containing a protease inhibitor (Roche, Basel, Switzerland) and phosphatase inhibitors (1 mM sodium fluoride, 1 mM β -glycerol phosphate, and 1 mM sodium vanadate) and were centrifuged at 10 000 *g* for 10 min. The supernatants (25 μ g protein) were subjected to western blot analysis of CYP2E1. To obtain nuclear extracts, liver tissues were prepared using the NE-PER Nuclear and Cytoplasmic Extraction Reagents kit (Thermo Fisher Scientific, Waltham, MA), according to the manufacturer's protocol. The nuclear extracts (20 μ g protein) were subjected to western blot analysis of HIF-1 α . Primary hepatocytes, cultured under a hypoxic conditions (1% O₂), were used as positive control (5 μ g) for western blotting of HIF-1 α . The samples were separated on SDS-polyacrylamide gels and transferred to polyvinylidene fluoride membranes using standard western blotting techniques. The membranes were incubated with an antibody against CYP2E1 (kindly provided by Dr Koichi Yoshinari (Tohoku University, Sendai, Japan)) at a dilution of 1:10 000 or with an antibody against HIF-1 α (NB100-449, Novus Biologicals, Littleton, CO) at a dilution of 1:1000. The CYP2E1 protein levels in the samples were normalized to those obtained with a glyceraldehyde-3-phosphate dehydrogenase antibody at a dilution of 1:10 000 (MAB374; Millipore, Billerica, MA, USA). The expression of HIF-1 α was normalized to the signal obtained with Coomassie brilliant blue staining.

Measurement of Hepatic CYP2E1 Activity *In Vitro*

Liver tissues (100 mg) were homogenized in 1 ml of ice-cold 50 mM potassium phosphate buffer (pH 7.4). The homogenate was centrifuged at 9000 g for 20 min. The supernatant was transferred to a new tube and centrifuged at 105 000 g for 60min. The pellet was suspended with 50 mM Tris-HCl (pH 7.4)/20% glycerol. The suspension was subjected to CYP2E1 activity assay with vivid CYP2E1 blue screening kit (Invitrogen).

Assessment of Cell Death and Viability in Primary-Cultured Mouse Hepatocytes

Cell death was analyzed with 1 µg/ml propidium iodide (Dojindo), which stains nuclei only when the cellular plasma membranes become permeabilized, and with Hoechst 33342 (Dojindo). Cell viability was determined using an MTT assay.¹⁷ The cell viability (%) of the test samples was calculated relative to that of the control sample.

Statistical Analysis

The statistical analysis was performed using Prism version 6.0 software (GraphPad Software, San Diego, CA, USA). A *P*-value < 0.05 was considered to indicate a significant difference.

RESULTS

Alleviation of APAP-Induced Liver Injury in *Cygb*-Null Mice

A single injection of APAP (300 mg/kg, i.p.) into C57Bl/6 mice induced significant liver injury, which was accompanied by a marked increase in the serum ALT levels (Supplementary Figure S1A) and a moderate to marked centrilobular necrosis (Supplementary Figure S1B) 6–12 h after the injection. Thus, in the subsequent experiments, wild-type and *Cygb*-null mice were killed 6 h after APAP injection.

The increase in serum ALT levels was significantly attenuated in the *Cygb*-null mice receiving APAP: the ALT levels of the wild-type and *Cygb*-null mice were $13\,970 \pm 2370$ and 4699 ± 1226 U/l, respectively (Figure 1a). In accordance with these results, the histological area of hepatocyte necrosis was diminished in the *Cygb*-null mice (Figure 1b). Relative necrotic area was larger in wild-type ($47.3 \pm 11.0\%$) than in *Cygb*-null mice ($17.8 \pm 5.0\%$) as shown in Figure 1c. The APAP-induced increase in the hepatic mRNA levels of chemokine (C-C motif) ligand 2 (*Ccl2*) in the *Cygb*-null mice was reduced to half of that detected in the wild-type mice. No differences in the hepatic mRNA expression levels of tumor necrosis factor α , interleukin 1 β , or interleukin 6 were observed between the wild-type and *Cygb*-null mice (Figure 1d). Hepatic GSH level in both mouse lines decreased dramatically at 2 h after APAP challenge. After the maximum depletion, hepatic GSH level in *Cygb*-null mice recovered quickly, compared with that in wild-type mice (Figure 1e). Three of the tested five wild-type mice showed low hepatic GSH level at 6 h after APAP injection, compared with *Cygb*-null mice (Figure 1f). Taken together, these results suggest that CYGB deficiency restrained APAP-induced acute liver injury.

Reduced Serum APAP Metabolites and Lower Hepatic O₂ Levels in *Cygb*-Null Mice

The hepatic expression of CYP2E1, an enzyme that generates NAPQI from APAP, was investigated in wild-type and *Cygb*-null mice. We confirmed previous reports indicating that hepatic CYP2E1 mRNA levels decreased in a time-dependent manner after APAP injection in wild-type mice (Supplementary Figure S1C).¹⁸ No differences were noted in the CYP2E1 mRNA and protein levels between untreated wild-type and *Cygb*-null mice (Figures 2a and b). After APAP challenge, similar decreases in the CYP2E1 mRNA and protein levels were observed in the wild-type and *Cygb*-null mice. Furthermore, the hepatic microsomal CYP2E1 activity *in vitro* was assessed. The Michaelis-Menten kinetics curve for the CYP2E1 activity of *Cygb*-null mice were almost same to that for the wild-type mice. In addition, the V_{max} and the K_m were 0.325 ± 0.10 nmol per mg protein/min and 17.48 ± 9.85 μ M for the wild-type mice, and 0.338 ± 0.03 nmol per mg protein/min and 19.72 ± 2.58 μ M for the *Cygb*-null mice, respectively. The differences between the wild-type and the *Cygb*-null mice were not observed (Figure 2c). However, the serum levels of CYP2E1-dependent APAP metabolites, ie, cysteinyl-APAP and *N*-acetyl-cysteinyl-APAP, which are derived from NAPQI (Figure 2d), were significantly decreased in the *Cygb*-null mice compared with the wild-type mice. In contrast, the APAP levels tended to be high in the *Cygb*-null mice and the levels of APAP-glucuronide, a CYP2E1-independent metabolite, remained unchanged (Figure 2e).

As O₂ is required for the CYP2E1-mediated NAPQI generation, we hypothesized that the livers of the *Cygb*-null mice had low concentrations of O₂ compared with the wild-type mice. To test this hypothesis, pimonidazole was used, which is frequently used to detect hypoxic regions in tissues.¹⁹ The resulting pimonidazole staining was limitedly positive around the central vein of the untreated livers. However, after treatment with APAP for 6 h, the pimonidazole-positive areas expanded to zone 2 (intermediate area) in the livers of the *Cygb*-null mice, but not in the wild-type mice (Figure 3a). Although HIF-1 α protein was not detected (Figure 3b), the data may support that CYGB deficiency results in decreased hepatic O₂ levels after APAP challenge.

Attenuation of APAP-Induced Cell Death in Primary-Cultured Mouse Hepatocytes by Hypoxia

Cultured primary mouse hepatocytes were challenged with 2.5–20 mM APAP under 5 or 20% O₂ for 16 h. The APAP challenge induced cell death in a dose-dependent manner under 20% O₂. Notably, the hepatocyte damage was significantly greater under 20% O₂ than under 5% O₂: when cells were treated with 20 mM APAP, the hepatocyte death in the presence of 20 and 5% O₂ was 67.0 and 31.8%, respectively (Figures 4a and b). In accordance with these results, cell viability after exposure to APAP was lower in the presence of 20% O₂ than in the presence of 5% O₂ (Figure 4c). HIF-1 α protein was detected in the presence of 1% O₂, but not in the presence of 5 and 20% O₂ (Figure 4d). These results demonstrated that the O₂ concentration influences the APAP toxicity in primary-cultured hepatocytes without HIF1 α activation.

Deterioration of the Viability of Primary-Cultured Mouse Hepatocytes by Co-Culture With HSCs Under APAP Treatment

Next, we studied whether the presence of HSCs influences the viability of mouse hepatocytes under conditions of APAP treatment. No difference in cell viability following APAP challenge was observed between wild-type and *Cygb*-null hepatocytes in monoculture under 5% O₂ (Figure 5a). However, hepatocytes co-cultured with wild-type HSCs showed significantly lower cell viability after APAP challenge compared with those co-cultured with *Cygb*-null HSCs: the cell viability values of hepatocytes in monoculture, those co-cultured with wild-type HSCs, and those co-cultured with *Cygb*-null HSCs were 0.29, 0.20, and 0.32, respectively (Figure 5b). In addition, hepatocytes showed a similar sensitivity to APAP when conditioned media from wild-type and *Cygb*-null HSCs were applied (Figure 5c). These results support the hypothesis that HSC-CYGB influences the behavior of hepatocytes, presumably through the O₂ supply.

Alleviation of CCL₄-Induced, but Not LPS/D-GalN- Induced, Acute Liver Injury By CYGB Deficiency

To investigate whether the mitigation of hepatocyte damage is unique to APAP in *Cygb*-null mice, two other acute liver injury models, ie, CCl₄-induced and LPS/D-GalN-induced liver damage, were employed. CCl₄ is metabolized by CYP2E1, similar to APAP. In contrast, LPS-induced liver injury is generally associated with Toll-like receptor 4 signaling pathways and is independent of CYP activity. In the CCl₄ model, the serum ALT levels were significantly higher in the wild-type mice (14 800 ± 1500 U/l) than in the *Cygb*- null mice (4340 ± 1030 U/l), similar to the APAP model (Figure 6a). The histologic analysis revealed that centri-lobular necrosis was more severe in the wild-type mice than in the *Cygb*-null mice (Figure 6b). In contrast, in the LPS/D- GalN model the serum ALT levels of the wild-type mice did not differ from those of the *Cygb*-null mice (333 ± 116 and 402 ± 189 U/l, respectively) (Figure 6c). A pathological analysis revealed the degeneration and necrosis of hepatocytes, the destruction of the hepatic architecture, and the presence of hemorrhage in both mouse strains (Figure 6d). These data support the hypothesis that CYGB deficiency decelerates the CYP2E1-mediated xenobiotic toxicity in the liver.

DISCUSSION

The current study demonstrated that APAP-induced liver injury was attenuated in *Cygb*-null mice compared with wild-type mice. CCl₄-induced liver injury was also alleviated in *Cygb*-null mice. APAP and CCl₄ toxicity is mediated through the production of reactive metabolites by CYP2E1. The hepatic CYP2E1 expression levels and in the *Cygb*-null mice were similar to those of the wild-type mice; nevertheless, the serum levels of NAPQI derivatives, such as cysteinyl-APAP and *N*-acetyl-cysteinyl-APAP, were lower in the *Cygb*-null mice than in the wild-type mice under APAP challenge. In addition, the serum APAP levels were elevated, albeit not significantly, in the *Cygb*-null mice compared with the wild-type mice. These results suggest that the generation of NAPQI is reduced in *Cygb*-null mice in the absence of changes in the hepatic CYP2E1 protein levels, and they support the theory that the enzymatic activity of CYP2E1 is attenuated in *Cygb*-null mice.

In this study, the hepatic microsomal CYP2E1 activity (under condition of disrupted sinusoidal microenvironment) in the *Cygb*-null mice was similar to that in the wild-type mice (Figure 2c). Considering that (1) CYPs are mono- oxygenases and (2) CYGB functions as an O₂-binding protein, we concluded that the APAP-derived toxicity may differ with regard to hepatic O₂ levels between *Cygb*-null and wild-type mice. In addition, pimonidazole-positive areas, indicating hypoxic conditions, were expanded only in the *Cygb*-null mice, although HIF1 α activation was not detected. As well as our observation, it has been reported that pimo- nidazole-positive cells are not always identical to HIF1 α -activated cells.^{20,21} Thus, we considered that the *Cygb*-null mice exhibited low O₂ tension in the liver, particularly after APAP challenge. Yan et al.⁵ showed that APAP-induced cell death in cultured mouse hepatocytes was attenuated in the presence of 10% O₂, which was accompanied by a decrease in mitochondrial oxidative stress. In the present study, we also observed that APAP-induced toxicity in mouse primary hepatocytes was alleviated even at lower O₂ levels (5% O₂). Surprisingly, co-culture with wild-type HSCs, but not with *Cygb*-null HSCs, exacerbated the APAP-induced hepatocyte death under a 5% O₂ atmosphere. In addition, conditioned media from wild-type HSCs and from *Cygb*-null HSCs failed to influence the APAP-induced hepatocyte death, indicating that stable components in these conditioned media, such as proteins and lipids, were ineffective. Although the co-culture system used in this study can't be said to reproduce perfectly the sinusoidal environment *in vivo*, these results indicate that the HSC-CYGB could affect APAP-induced hepatocyte injury.

The O₂ affinity of CYGB has been reported to be equivalent to that of myoglobin and neuroglobin, and is considerably higher than that of hemoglobin.⁶ This fact suggests that CYGB releases O₂ at lower O₂ tension compared with hemoglobin and, in combination, (1) HIF1 α protein was detected in the hepatocytes cultured with 1% O₂ but not in that with 20 and 5% O₂; (2) in fact, the wild-type HSCs, but not *Cygb*-null HSCs, can accelerate the APAP hepatocyte injury under 5% O₂; CYGB may be an early sensor for low oxygen level and supply O₂ to neighboring cells before falling in hypoxia (activation of HIF). In other words, CYGB can have a role in O₂ supply after the consumption of O₂ derived from hemoglobin *in vivo*. When excess CYP2E1 metabolism causes a shortage of O₂ in hepatocytes, the HSC-CYGB may supply O₂ temporarily and locally to hepatocytes during the O₂ insufficiency.

It has been reported that APAP damages the hepatic microvasculature, which precedes hepatocellular injury. *In vivo* microscopy indicated that this damage consists of endothelial cell swelling and the penetration of erythrocytes into the space of Disse. Significant decreases in the blood supply in hepatic sinusoids were observed 2 and 6h after APAP administration.²² In contrast, when HSCs become activated, they undergo changes in the cytoskeletal machinery and gain the ability to contract.²³ Some studies have demonstrated that activated HSCs contract in response to various agents.^{24,25} Thus, activated HSCs are thought to be involved in the disturbance of hepatic microcirculation.²⁶ A previous study reported that CYGB was able to suppress HSC activation.²⁷ Considering all of these reports, the loss of CYGB may lead to the 'priming' of HSCs to the activated stage and can cause immediate sinusoidal constriction after APAP challenge due to HSC contraction. However,

the hypothesis could be denied, because *Cygb*-null mice did not show attenuated LPS-induced liver injury.

In conclusion, the present study demonstrated in part that APAP-induced acute liver injury was attenuated in *Cygb*-null mice, presumably due to local low O₂ level (but not hypoxia) around hepatocytes closely adherent to HSCs (Figure 7). Although the molecular mechanism of O₂ transfer from HSCs to hepatocytes remains uncharacterized, this study provides important evidence to further understand the molecular mechanism of drug-induced liver injury mediated by CYP2E1.

Supplementary Material

Refer to Web version on PubMed Central for supplementary material.

ACKNOWLEDGMENTS

We thank Ms Chiho Kadono for animal care, and Dr Wenhao Cui, Dr Keiko Iwaisako, and Dr Kazuki Nakatani (Osaka City University) for their valuable discussion and comments on this study. This investigation was supported in part by a Grant-in-Aid for Scientific Research (B) from the Japan Society for the Promotion of Science (JSPS) through grant 25293177 (to NK) (2013–2016), the Mochida Memorial Foundation (to TM), and the National Cancer Institute Intramural Research Program (to FJG).

References

1. Lieber CS. Cytochrome P-4502E1: its physiological and pathological role. *Physiol Rev* 1997;77:517–544. [PubMed: 9114822]
2. Gonzalez FJ. The 2006 Bernard B. Brodie Award Lecture. Cyp2e1. *Drug Metab Dispos* 2007;35:1–8. [PubMed: 17020953]
3. Gonzalez FJ, Kimura S. Study of P450 function using gene knockout and transgenic mice. *Arch Biochem Biophys* 2003;409:153–158. [PubMed: 12464254]
4. Chen C, Krausz KW, Idle JR, et al. Identification of novel toxicity-associated metabolites by metabolomics and mass isotopomer analysis of acetaminophen metabolism in wild-type and Cyp2e1-null mice. *J Biol Chem* 2008;283:4543–4559. [PubMed: 18093979]
5. Yan HM, Ramachandran A, Bajt ML, et al. The oxygen tension modulates acetaminophen-induced mitochondrial oxidant stress and cell injury in cultured hepatocytes. *Toxicol Sci* 2010;117:515–523. [PubMed: 20616211]
6. Hankeln T, Ebner B, Fuchs C, et al. Neuroglobin and cytoglobin in search of their role in the vertebrate globin family. *J Inorg Biochem* 2005;99:110–119. [PubMed: 15598495]
7. Tosqui P, Colombo MF. Neuroglobin and cytoglobin: two new members of globin family. *Rev Bras Hematol Hemoter* 2011;33:307–311. [PubMed: 23049323]
8. Avivi A, Gerlach F, Joel A, et al. Neuroglobin, cytoglobin, and myoglobin contribute to hypoxia adaptation of the subterranean mole rat *Spalax*. *Proc Natl Acad Sci USA* 2010;107:21570–21575. [PubMed: 21115824]
9. Nakatani K, Okuyama H, Shimahara Y, et al. Cytoglobin/STAP, its unique localization in splanchnic fibroblast-like cells and function in organ fibrogenesis. *Lab Invest* 2004;84:91–101. [PubMed: 14647402]
10. Schmidt M, Gerlach F, Avivi A, et al. Cytoglobin is a respiratory protein in connective tissue and neurons, which is up-regulated by hypoxia. *J Biol Chem* 2004;279:8063–8069. [PubMed: 14660570]
11. Oleksiewicz U, Liloglou T, Field JK, et al. Cytoglobin: biochemical, functional and clinical perspective of the newest member of the globin family. *Cell Mol Life Sci* 2011;68:3869–3883. [PubMed: 21744065]

12. Kawada N, Kristensen DB, Asahina K, et al. Characterization of a stellate cell activation-associated protein (STAP) with peroxidase activity found in rat hepatic stellate cells. *J Biol Chem* 2001;276:25318–25323. [PubMed: 11320098]
13. Mabuchi A, Mullaney I, Sheard PW, et al. Role of hepatic stellate cell/ hepatocyte interaction and activation of hepatic stellate cells in the early phase of liver regeneration in the rat. *J Hepatol* 2004;40:910–916. [PubMed: 15158330]
14. Yin C, Evason KJ, Asahina K, et al. Hepatic stellate cells in liver development, regeneration, and cancer. *J Clin Invest* 2013;123:1902–1910. [PubMed: 23635788]
15. Thuy le TT, Morita T, Yoshida K, et al. Promotion of liver and lung tumorigenesis in DEN-treated cytoglobin-deficient mice. *Am J Pathol* 2011;179:1050–1060. [PubMed: 21684245]
16. Iwaisako K, Hatano E, Taura K, et al. Loss of Sept4 exacerbates liver fibrosis through the dysregulation of hepatic stellate cells. *J Hepatol* 2008;49:768–778. [PubMed: 18804890]
17. da Rosa EJ, da Silva MH, Carvalho NR, et al. Reduction of acute hepatic damage induced by acetaminophen after treatment with diphenyl diselenide in mice. *Toxicol Pathol* 2012;40:605–613. [PubMed: 22301948]
18. Ishibe T, Kimura A, Ishida Y, et al. Reduced acetaminophen-induced liver injury in mice by genetic disruption of IL-1 receptor antagonist. *Lab Invest* 2009;89:68–79. [PubMed: 19002106]
19. Samoszuk MK, Walter J, Mechetner E. Improved immunohistochemical method for detecting hypoxia gradients in mouse tissues and tumors. *J Histochem Cytochem* 2004;52:837–839. [PubMed: 15150293]
20. Harada H, Inoue M, Itasaka S, et al. Corrigendum: Cancer cells that survive radiation therapy acquire HIF-1 activity and translocate toward tumour blood vessels. *Nat Commun* 2013;4:2314.
21. Tanaka H, Yamamoto M, Hashimoto N, et al. Hypoxia-independent overexpression of hypoxia-inducible factor 1alpha as an early change in mouse hepatocarcinogenesis. *Cancer Res* 2006;66:11263–11270. [PubMed: 17145871]
22. Hinson JA, Roberts DW, James LP. Mechanisms of acetaminophen- induced liver necrosis. *Handb Exp Pharmacol* 2010:369–405.
23. Jiang JX, Torok NJ. Liver Injury and the Activation of the Hepatic Myofibroblasts. *Curr Pathobiol Rep* 2013;1:215–223. [PubMed: 23977452]
24. Friedman SL. Hepatic stellate cells: protean, multifunctional, and enigmatic cells of the liver. *Physiol Rev* 2008;88:125–172. [PubMed: 18195085]
25. Reynaert H, Thompson MG, Thomas T, et al. Hepatic stellate cells: role in microcirculation and pathophysiology of portal hypertension. *Gut* 2002;50:571–581. [PubMed: 11889082]
26. Vollmar B, Menger MD. The hepatic microcirculation: mechanistic contributions and therapeutic targets in liver injury and repair. *Physiol Rev* 2009;89:1269–1339. [PubMed: 19789382]
27. Cui W, Wang M, Maegawa H, et al. Inhibition of the activation of hepatic stellate cells by arundic acid via the induction of cytoglobin. *Biochem Biophys Res Commun* 2012;425:642–648. [PubMed: 22850540]

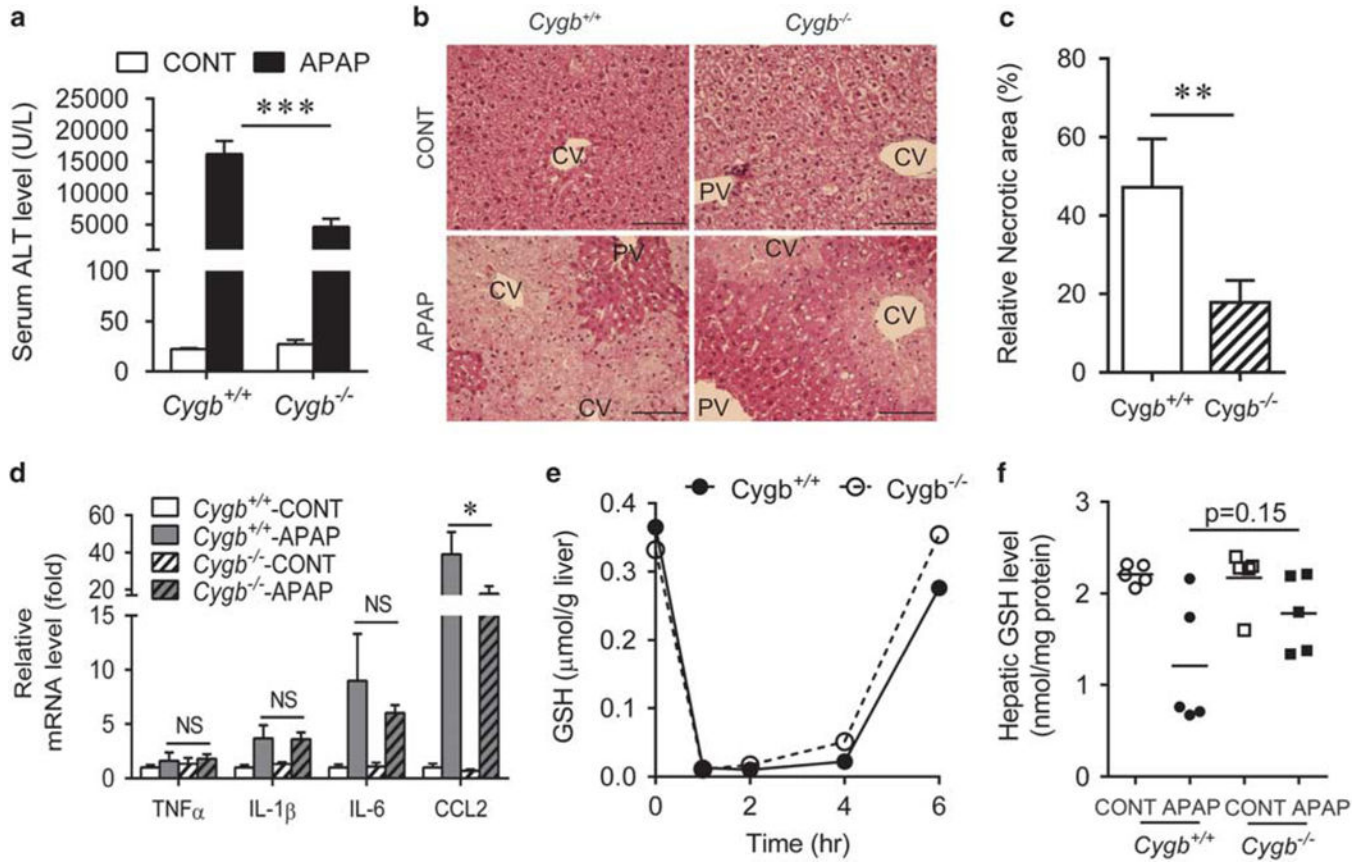
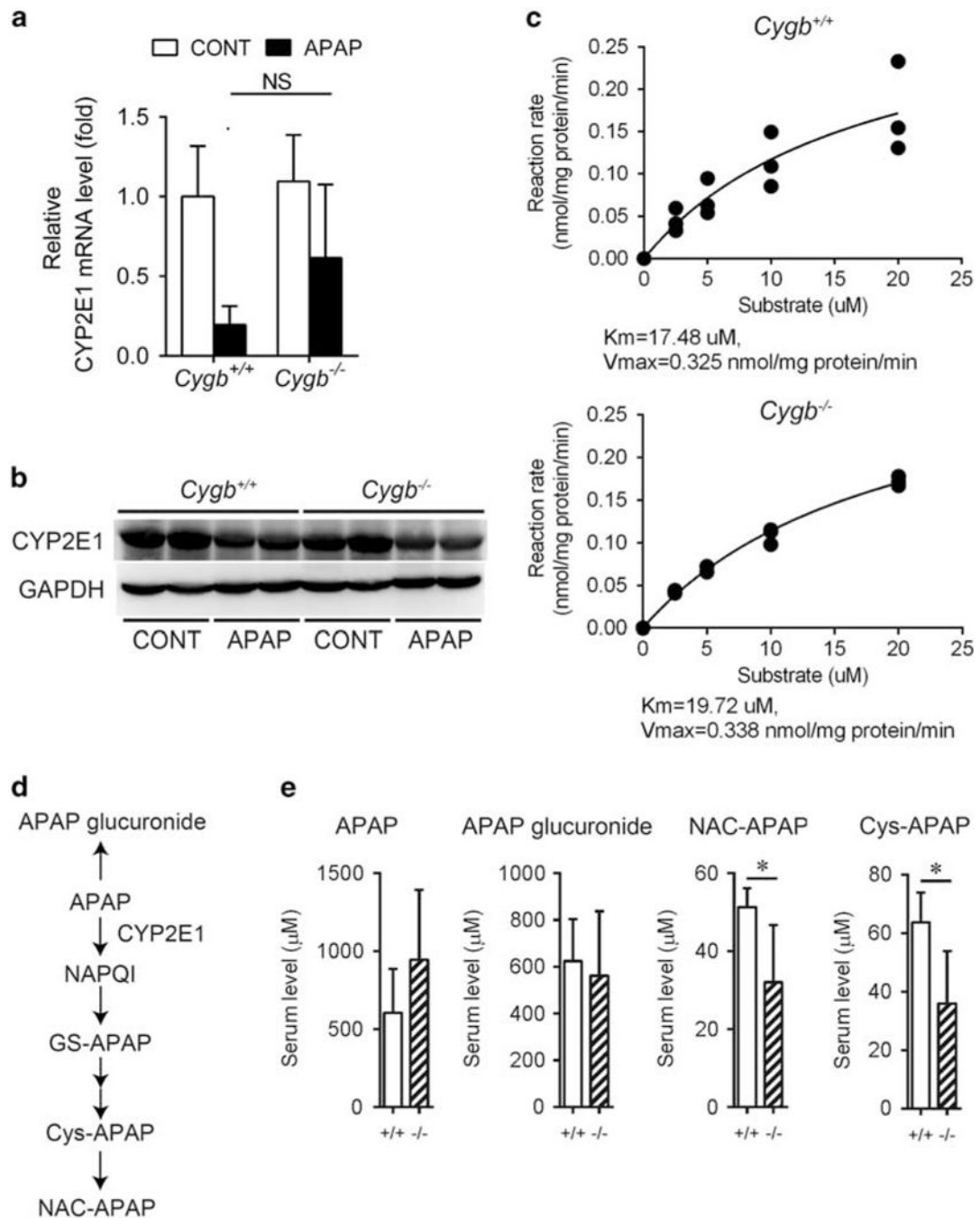


Figure 1. Analysis of *N*-acetyl-*p*-aminophenol (APAP)-induced acute liver injury in wild-type and cytoglobin (*Cygb*)-null mice. **(a)** Serum alanine aminotransferase (ALT) levels. ALT activity was measured 6h after saline (CONT) or 300 mg/kg APAP administration. Each bar represents the mean value and s.d. ($n = 5-6$). **(b)** Representative liver sections stained with hematoxylin and eosin ($\times 400$, bar = 100 μ m). CV, central vein. PV, portal vein. **(c)** Relative necrotic area was represented by the percentage ratio of necrotic area to liver area. Each bar represents the mean value and s.d. ($n = 5$). **(d)** Quantitative reverse transcription-PCR analysis of tumor necrosis factor- α (*TNF- α*), interleukin (*IL*)-1 β , *IL*-6, and chemokine (C-C motif) ligand 2 (*Ccl2*) mRNAs during APAP-induced liver injury. Each bar represents the mean value and s.d. ($n = 5-6$). **(e)** Time course of glutathione (GSH) levels in the liver ($n = 2$). **(f)** Hepatic GSH level at 6h. Each bar represents the mean value ($n = 5$). Wild-type and *Cygb*-null mice are designated *Cygb*^{+/+} and *Cygb*^{-/-}, respectively. Significance was determined by a one-way ANOVA with Bonferroni's test. * $P < 0.05$, *** $P < 0.001$; NS, not significant.

**Figure 2.**

Cytochrome P450, family 2, subfamily E, polypeptide 1 (CYP2E1) expression and *N*-acetyl-*p*-aminophenol (APAP) metabolism in the liver. Quantitative reverse transcription-PCR (a) and western blot (b) analyses of CYP2E1 expression in the liver 6h after APAP. Each bar represents the mean value and s.d. ($n = 5-6$). Significance was determined by a one-way ANOVA with Bonferroni's test (NS, not significant). (c) Major *in vivo* APAP metabolic pathways are indicated. GS-APAP, 3-gultathionyl-APAP; Cys-APAP, cysteinyl-APAP; NAC-APAP, *N*-acetyl-cysteinyl-APAP. (d) Serum levels of APAP and its major metabolites in

Cygb^{+/+} and *Cygb*^{-/-} mice. Serum samples were collected 2h after the administration of APAP, and APAP metabolites were measured by a liquid chromatography-mass spectrometry (LC-MS) analysis. The values are expressed as the relative abundance (mean and s.d., $n = 5$). Significance was determined using an unpaired f-test ($*P < 0.05$). (e) Hepatic microsomal CYP2E1 activity. The reaction rate was determined as described in Materials and Methods.

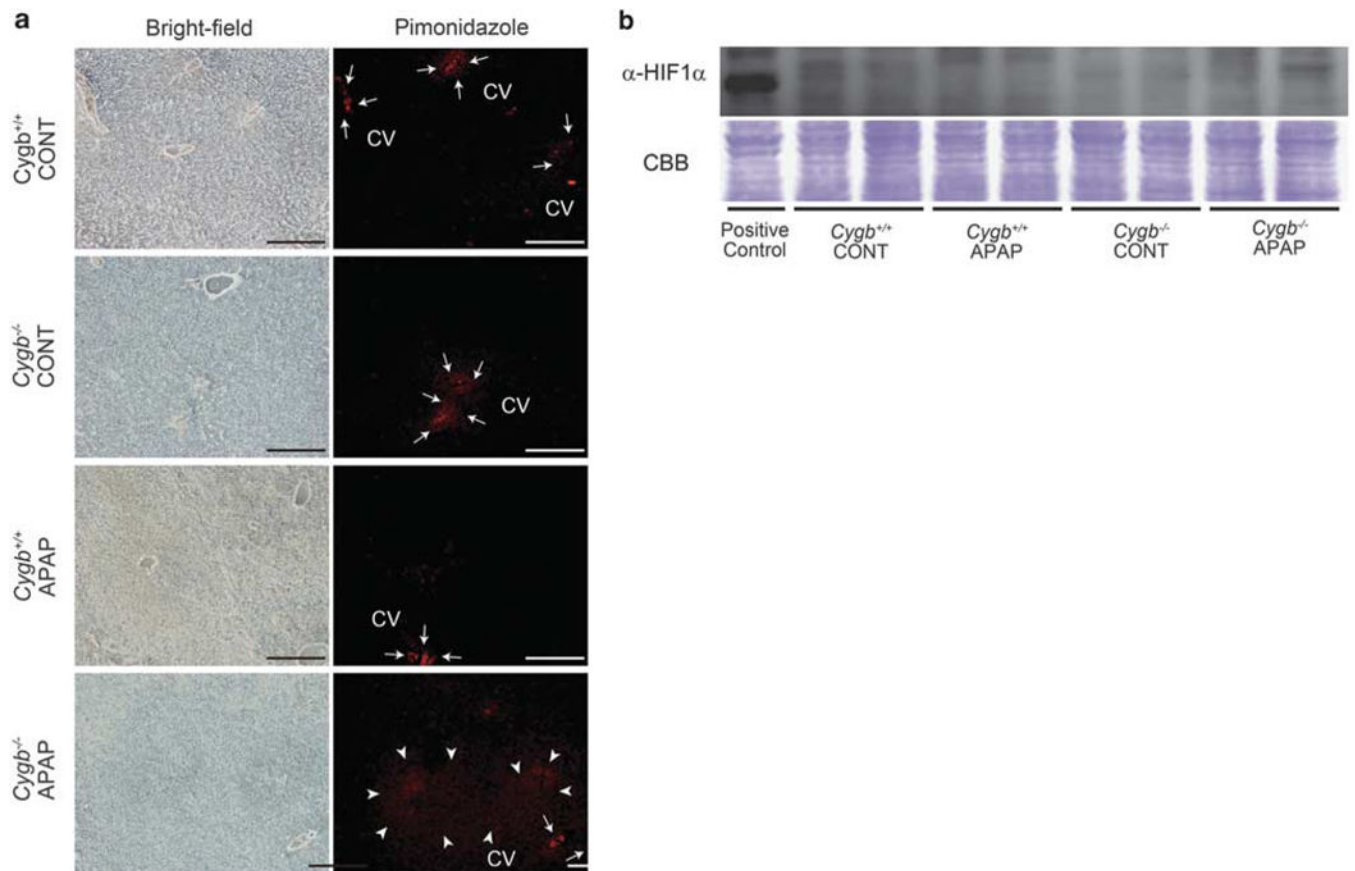
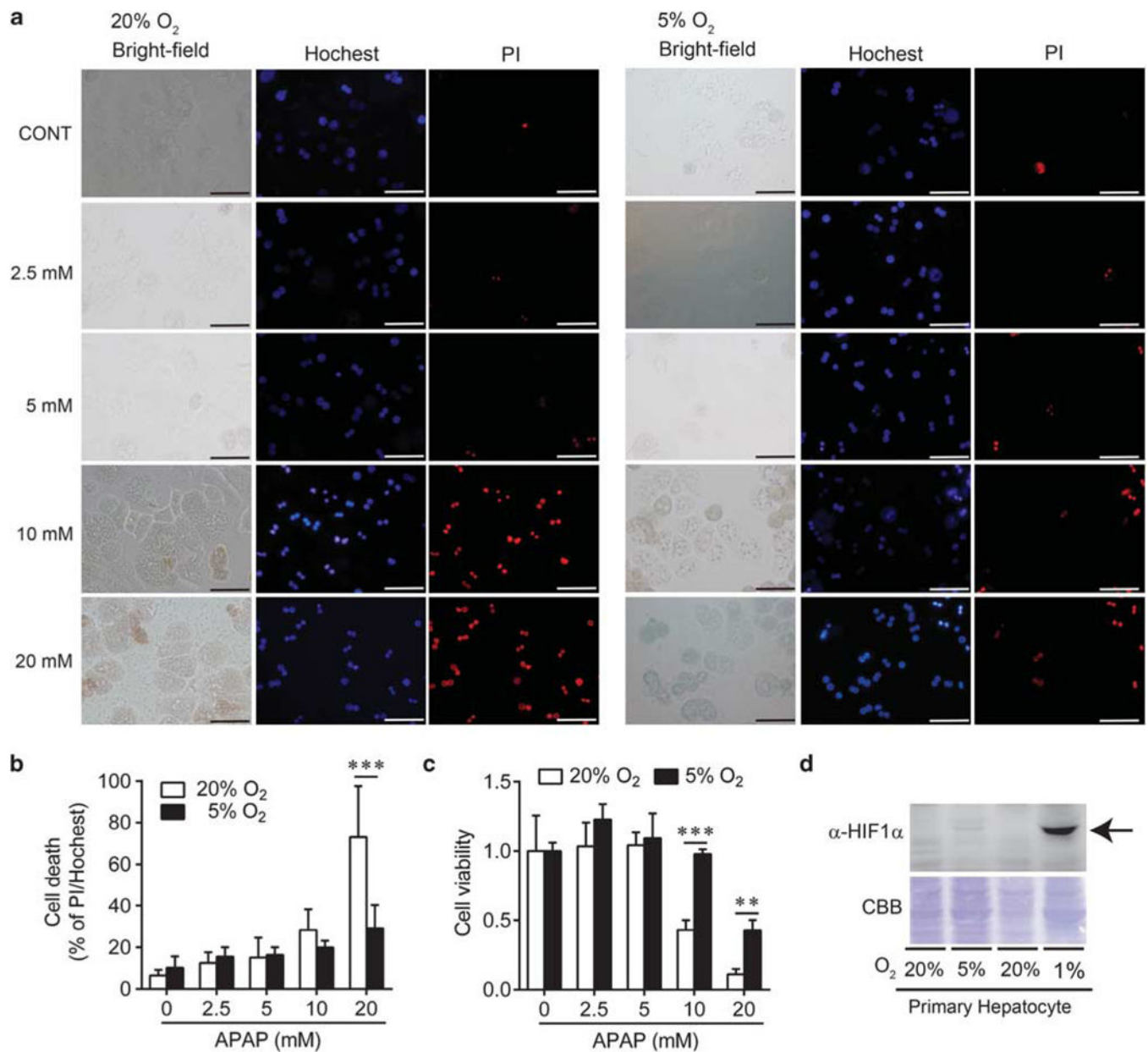


Figure 3. Determination of hypoxic conditions in mouse liver. **(a)** Pimonidazole staining in the livers of *cytoglobin* (*Cygb*)^{+/+} (left) and *Cygb*^{-/-} (right) mice 6h after APAP treatment. Arrowheads indicate pimonidazole-positive areas. Arrows indicate the central vein (CV) (x 100, bar = 200 μm). **(b)** Western blotting of hypoxia-inducible factor 1α (HIF-1α) protein. Coomassie brilliant blue (CBB) staining was used for the normalization.

**Figure 4.**

Influence of oxygen level on *N*-acetyl-*p*-aminophenol (APAP)-induced hepatocyte injury in culture. **(a)** Representative images of APAP-induced hepatocyte damage. Cell death was determined using propidium iodide (PI) staining under 5 or 20% oxygen (O₂) 16 h after APAP administration. The concentrations of APAP were 0, 2.5, 5, 10, and 20 mM. Stained hepatocytes were observed under bright-field (left) and dark-field microscopy (center, Hoechst 33342; right, PI; x 400, bar = 50 μm). **(b)** Determination of cell death calculated as the ratio of PI-positive hepatocytes under 5 or 20% O₂. The values represent the percentage ratio of PI-positive hepatocytes to Hoechst-positive hepatocytes ($n = 4-8$). **(c)** Determination of cell viability by an MTT assay. Significance was determined by a two-way ANOVA with Bonferroni's test (**b** and **c**). ** $P < 0.01$, *** $P < 0.001$. **(d)** Western blotting of HIF-1α protein

under conditions of 1, 5, and 20% O₂. Arrow indicated HIF-1a protein. Coomassie brilliant blue (CBB) staining was used for the normalization.

Author Manuscript

Author Manuscript

Author Manuscript

Author Manuscript

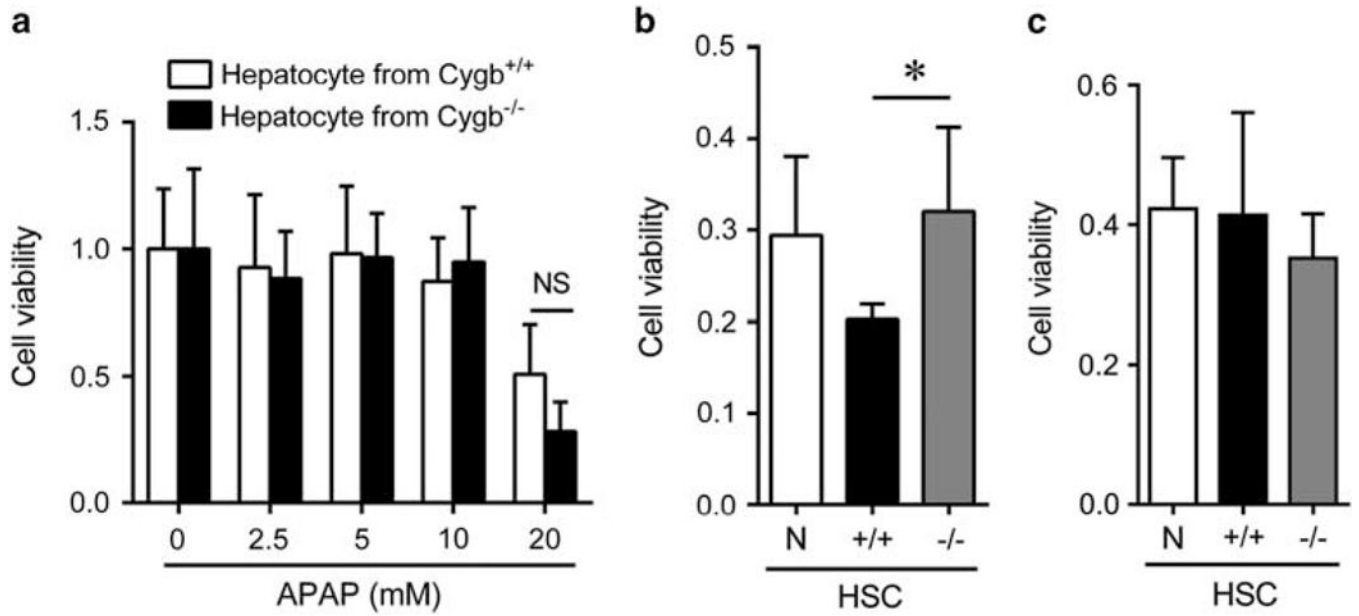


Figure 5. Presence of HSCs deteriorates the viability of mouse hepatocytes under conditions of APAP treatment. **(a)** Comparison of cell viability 16h after APAP challenge between cytoglobin (*Cygb*)^{+/+} and *Cygb*^{-/-} hepatocytes. **(b)** Effect of HSCs isolated from *Cygb*^{+/+} or *Cygb*^{-/-} mice on hepatocyte viability after 30mM APAP challenge for 16h at low oxygen level (5% oxygen (O₂)). White, black, and gray column indicate without HSCs, with *Cygb*^{+/+} HSCs, and with *Cygb*^{-/-} HSCs, respectively. **(c)** Effects of HSC conditioned media on hepatocyte viability after 30mM APAP challenge. Conditioned media were prepared as described in the Materials and Methods section. White, black, and gray columns indicate culture in the absence of conditioned medium, in the presence of conditioned medium from *Cygb*^{+/+} HSCs, and in the presence of conditioned medium from *Cygb*^{-/-} HSCs, respectively. Significance was determined by a two-way ANOVA with Bonferroni's test **(a)** and a one-way ANOVA with Bonferroni's test **(b and c)**. **P* < 0.05; NS, not significant.

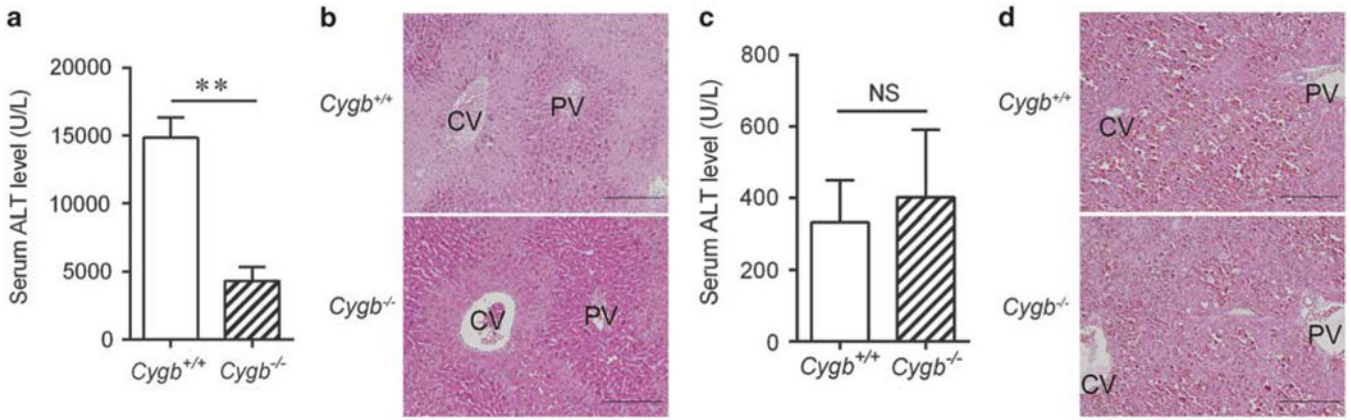


Figure 6. Carbon tetrachloride (CCl₄)-induced and lipopolysaccharide (LPS)/D-galactosamine (D-GalN)-induced acute liver injury in mice. **(a and b)** Acute liver injury induced by 0.5 mg/kg CCl₄ administration. Serum alanine aminotransferase (ALT) activity **(a)** and liver histology **(b; x 200, bar = 100 μm)** 24 h after CCl₄ injection are shown (each, *n* = 3–4). CV, central vein; PV, portal vein. **(c and d)** Acute liver injury induced by 700 mg/kg of D-GalN and 5 μg/kg of LPS. Serum ALT activity **(c)** and liver histology **(d; x 200, bar = 100 μm)** 6h after LPS/D-GalN injection are shown (each, *n* = 10). CV, central vein; PV, portal vein. Significance was determined by an unpaired *t*-test (***P* < 0.01; NS, not significant).

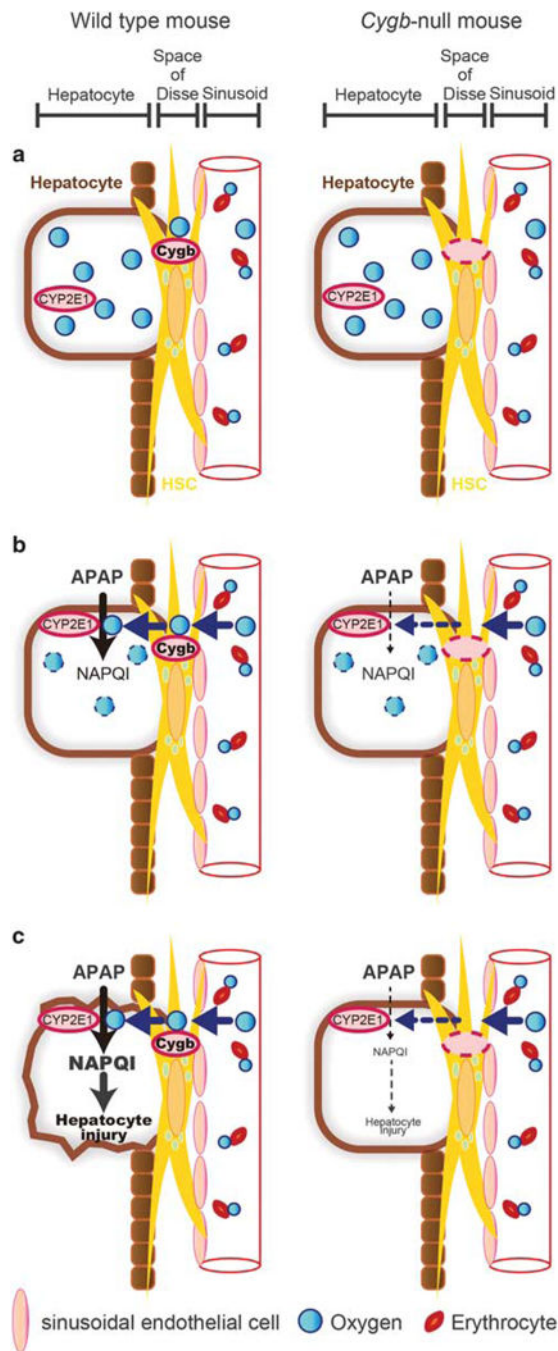


Figure 7. Putative mechanism by which hepatic stellate cell (HSC)- expressed cytoglobin (CYGB) is involved in *N*-acetyl-*p*-aminophenol (APAP)-induced liver injury. **(a)** The oxygen (O₂) concentration in the livers of *Cygb*-null mice was similar to that of wild-type mice under normal conditions. **(b)** At high APAP concentrations, APAP is metabolized by CYP2E1 and O₂ is rapidly consumed. As a result, hepatocytes tend to be temporarily O₂ deficient. O₂ would be supplied from CYGB in HSCs located in the space of Disse in wild-type mice, but this is not the case in *Cygb*-null mice. **(c)** Thus, CYP2E1 efficiently generates *N*-acetyl-*p*-

benzoquinone imine (NAPQI) from APAP in wild-type mice. In contrast, in *Cygb*-null mice NAPQI production is decreased because of impaired local O₂ supply from HSCs; thus, NAPQI-dependent hepatocyte injury is attenuated. Blue arrows indicate O₂ transfer. Bold black arrows indicate the pathway by which APAP toxicity is mediated. Dashed line arrows indicate reduction.